CHAPTER 3

Effect of the hockey stick-shaped mesogen as an additive on the critical behavior at the isotropic to nematic and nematic to smectic-*A* phase transitions in octyloxy-cyano-biphenyl

3.1. Introduction

Fundamental mesogenic behavior of liquid crystalline compounds depends on their molecular structure and relative organization in mesophases. So far a number of mesogenic compounds displaying a variety of mesophases with diverse molecular ordering and phase structure have been synthesised and comprehensively studied. Some of them are of further interest due to their exclusive molecular behavior within such mesophases as well as at the transitions between them. In that sense, the bent-core or banana-shaped compounds have emerged as a field of significant interest in liquid crystal research. Apart from the interest on molecular behavior and appearance of different unique mesophases in bent-core liquid crystals, mixtures of such compounds with rod-like molecules, exhibiting exciting mesophase transitions including those usually appeared for only single calamitic compounds, are also much attractive for their unpredictable varying characteristics. Properties such as enhancement of chirality in cholesteric [1,2] and smectic-C^* fluids [3], generation of antiferroelectric order in smectics [4-7], induction of novel smectic phases [8], inimitable temperature dependence of elastic constant [9-11] or nanophase segregations [12,13] of such mixtures of rod-like and bent-core liquid crystal brought them at the center of scientific attention and stimulates considerable research efforts regarding formulation and characterization of noble liquid crystalline mixtures.

In the past few decades, several experimental and theoretical efforts have been devoted to extract the exact order character of the isotropic to nematic ($I-N$) phase transition. Considering the mean-field approach, Landau and de Gennes [14] explained the $I-N$ phase transition by assuming the free energy density in powers of the nematic order parameter S(T). However, the mean-field theory [15] cannot describe the critical phenomena at very close to the transition. A number of diverse experimental techniques have been reported so far to analyze this critical region as well as to disclose the unique aspects of

the *I*−*N* phase transition. However, none of the experimental techniques have been able to describe a complete picture regarding the nature of this transition. Besides a few disagreements, most of them reveal a tricritical nature [16–18] for the *I*−*N* phase transition which again can be explained in the context of Landau-de Gennes theory with the free energy density expanded up to sixth order in powers of the nematic order parameter S(*T*).

Moreover, in case of nematic−smectic-*A* (*N*−Sm-*A*) phase transition a number of experimental attempts have been employed so far but it still remains only partially understood. On the basis of mean-field model, Kobayashi [19] and McMillan [20] suggested that depending upon the McMillan ratio (T_{NA}/T_{IN}, where T_{NA} and T_{IN} are the *N*−Sm-*A* and *I*−*N* phase transition temperatures respectively), the *N*−Sm-*A* phase transition can either be a first order or second order along with the existence of a tricritical point (TCP) where the transition undertakes a crossover from second order to first order in nature. With the introduction of a modified functional, de Gennes [14,21] further proposed a concept of coupling in between the nematic (S) and smectic (Ψ) order parameters, which predicts the transition to be in the 3D-*XY* universality class. However, experimental evidences indicate a strong dependence of that transition on the width of the nematic range, which shows that a wide nematic width signifies a weak coupling between the nematic and smectic order parameter, thus making the *N*−Sm-*A* transition to be second order in nature, while for a sufficiently small nematic width, indicating a stronger coupling between S and Ψ, drives the transition to first order character. Although theoretically the tricritical limit is expected for a McMillan ratio of 0.87, experimental observations demonstrate somewhat higher values, ranging from 0.942 to 0.994 [22-28]. So the non-universal type behavior has been observed in a number of cases, *i.e.*, the 3D-*XY* appearance can be feasible only when the nematic order is completely saturated [29-32]. Furthermore, Halperin, Lubensky and Ma (HLM) [33] by introducing a correction in the free energy

term ~ Ψ^3, have shown that the *N*−Sm-*A* transition is always weakly first order in nature because of the presence of the coupling between the nematic director fluctuations and smectic order parameter. Therefore, the concept of tricritical point (TCP) is ruled out in this case. So far, a number of experimental techniques such as specific heat capacity measurements, dielectric techniques, x-ray diffraction measurements *etc.*, have widely been used to study the nature of this phase transition in several rod-like liquid crystals having a variety of core structures as well as in their mixtures. However, transitional phenomena in mixtures involving rod-like and bent-core mesogens are relatively less investigated, even though they may prove to be helpful in extracting valuable information regarding transitional anomaly and order character of a transition.

In this chapter, a systematic investigation of the critical behavior in the vicinity of the *I*−*N* and *N*−Sm-*A* phase transitions has been reported in a few binary liquid crystalline mixtures consisting of a hockey stick-shaped compound, 4-(3-decyloxyphenyliminomethyl) phenyl 4-decyloxycinnamate (SF7) and the calamitic compound, 4′-octyloxy-4-cyanobiphenyl (8OCB) from a quite high-resolution (in both the birefringence and temperature) measurement of optical birefringence (Δn). An effective order parameter critical exponent (β) value has been extracted by investigating the critical fluctuation near the *I*–*N* phase transition. From an analysis of the temperature derivative of Δn data in the vicinity of *N*−Sm-*A* phase transitions, power-law behavior with a characteristic effective heat capacity critical exponent (α') has been determined and compared with the available literature data. The effective critical exponent (α') has also been investigated along the path of variation for the dopant concentration. The observed pretransitional behavior is discussed in the light of crossover behavior under the consideration of effect of the hockey stick-shaped molecules on the resultant molecular order in the host medium. Moreover, an order parameter critical exponent (β') has been extracted in the vicinity of *N*−Sm-*A* phase transition for all of the studied mixtures.

3.2. Materials

The hockey stick-shaped compound, 4-(3-decyloxyphenyliminomethyl) phenyl 4-decyloxycinnamate (SF7) was synthesized and purified at the Institute of Physical Chemistry, Martin Luther University, Halle, Germany and the compound 4′-octyloxy-4-cyanobiphenyl (8OCB) was purchased from E. Merck, UK (having purity higher than 99.9%) and were used without further purification. The structural formulae and transition scheme for both the pure compounds are given in Fig. 3.1. Several mixtures have been prepared with different molar concentrations (x_{SF7} = 0.012, 0.03, 0.05 and 0.065) by adding small amounts of the hockey stick-shaped compound into the host rod-like mesogen. The textures of the samples were observed under a polarizing optical microscope (BANBROS) equipped with INSTEC HCS302 hot stage, controlled by INSTEC mK1000 thermo system.

Compound 1

(a)

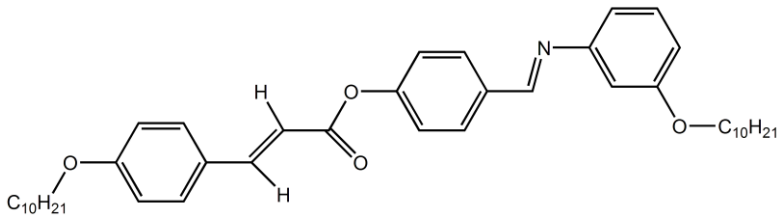

Cr (350 K) **Sm-*C*$_a$** (361 K) **Sm-*C*$_s$** (371.5 K) **Sm-*A*** (374 K) ***I***

Compound 2

(b)

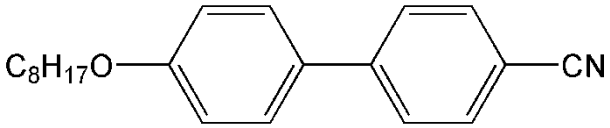

Cr (327.5 K) **Sm-*A*$_d$** (340 K) ***N*** (353 K) ***I***

Figure 3.1. Chemical structure and phase behavior of (a) the hockey stick-shaped compound (SF7) and (b) the rod-like compound (8OCB).

3.3. Phase diagram

The phase diagram of the binary system consisting of SF7 and 8OCB for four different concentrations along with that of pure 8OCB, as obtained from

both the polarizing optical microscopy and the optical transmission technique has been illustrated in Fig. 3.2. The pure rod-like compound 8OCB shows the stable phase sequence *I*–Sm-A_d–*N*–Cr as being cooled from isotropic state. Here, Sm-A_d refers to smectic-*A* phase with partial bi-layer structure [the layer thickness (*l*) is intermediate between the molecular length (d) and twice the molecular length]. Conversely, the pure hockey stick-shaped compound (SF7) shows two polymorphic tilted smectic phases - the synclinic smectic-*C* (Sm-C_s) as well as the anticlinic smectic-*C* (Sm-C_a) phases along with a Sm-*A* phase, appearing in a relatively small temperature range (~2.5 K) [34].

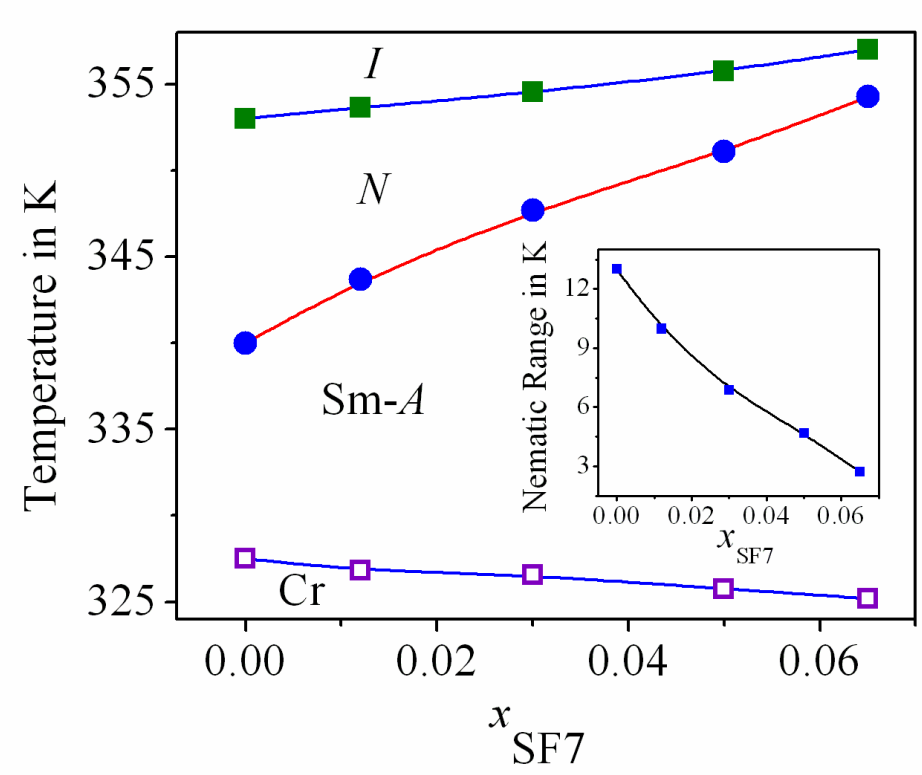

Figure 3.2. Phase diagram for the binary mixture consisting of SF7 and 8OCB. x_{SF7} denotes the mole fraction of SF7. *I* – isotropic phase, *N* – nematic phase and Sm-*A* – smectic-*A* phase. ■: *I*–*N* transition temperature; ●: *N*–Sm-*A* transition temperature; □: Melting temperatures measured during heating cycle. Inset depicts variation of nematic range with concentration for the present system. Solid lines are drawn for guidance to eye.

In these binary mixtures, particular focus has been taken on the region where the concentration of the guest compound, *i.e.*, hockey stick-shaped

compound (SF7) is less compared to that of the rod-like host compound (8OCB). It has been observed that by addition of a small amount of the hockey stick-shaped compound in the host mesogenic system has a significant influence on both the *I*−*N* (T_{IN}) and *N*−Sm-*A* (T_{NA}) transition temperatures. Further both T_{IN} and T_{NA} shows an increasing trend when plotted against concentration of SF7 with the phase boundary between the Sm-*A* and *N* phases being relatively steeper than that between the *N* and *I* phases and thus resulting a decrease in the nematic width. This again signifies a destabilization of the nematic phase in the host medium caused by the angular mesogenic compound. The variation of the nematic range against molar concentration is also presented in the inset of Fig. 3.2. The nematic range has been found to decrease from a value of 13 K to near about 3 K for the studied mixtures, where the shrinkage follows a nearly linear trend with the variation of molar concentration.

3.4. Optical birefringence measurements

3.4.1. Optical transmission (OT) technique

The high-resolution optical birefringence ($\Delta n = n_e - n_o$) data has been accomplished by measuring the optical phase retardation [35-38] of a laser beam (λ = 632.8 nm) through a homogeneously aligned ITO-coated liquid crystal cell of all the binary mixtures along with pure 8OCB compound. The obtained experimental data for the investigated system has been represented in Fig. 3.3. At the *I*−*N* transition, the temperature dependence of birefringence (Δn) demonstrates a sharp change, indicating a first-order nature of that transition. On further cooling, well within the nematic phase, the Δn value continues to increase with decrease in temperature which again follows a more or less identical pattern for all the mixtures under study. Such a change is in effect due to the enhancement of molecular ordering in the mesogenic medium with decreasing temperature. Moreover, it has been noticed that all the Δn vs. temperature curves are accompanied with a small but finite measurable

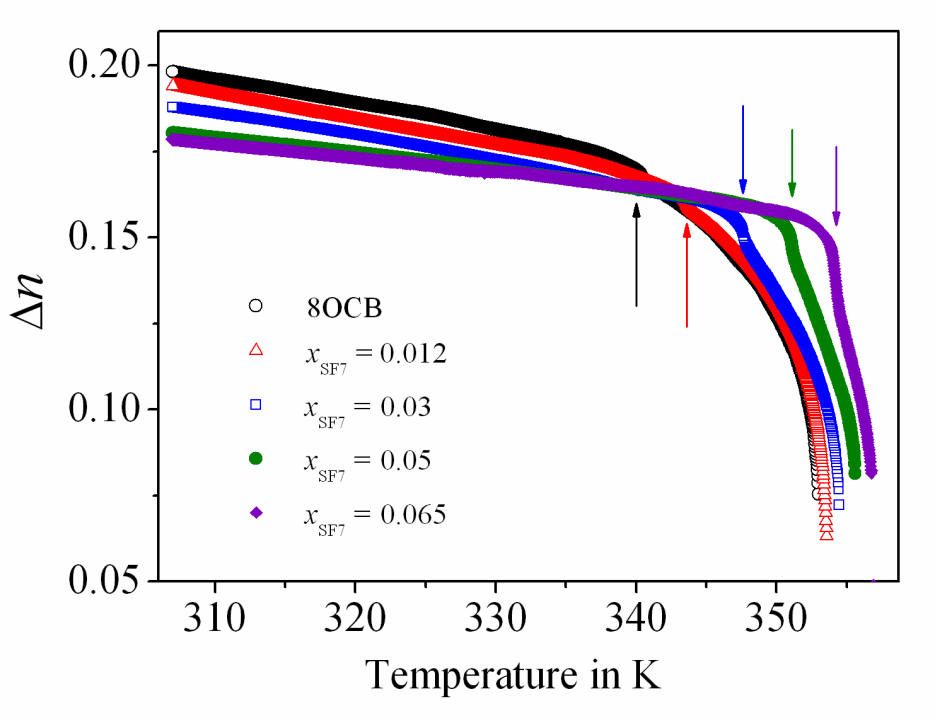

Figure 3.3. Temperature dependence of optical birefringence (Δ*n*) data for all the mixtures along with that for pure 8OCB. Vertical arrows show the *N*−Sm-*A* phase transition for all the mixtures.

change in Δ*n* on entering the low temperature Sm-*A* phase, which again is due to the development of additional translational ordering. A quite visible pretransitional behavior has been observed in the Δ*n* curve within the nematic phase in the range of 2.2 K to 4.9 K, prior to the *N*−Sm-*A* phase transition. Such an influence is owing to the coupling between the nematic and smectic-*A* order parameters. Moreover, this coupling becomes stronger with shrinkage in the nematic width [39]. So in this case, by varying the concentration of SF7 in the host mesogen, the width of the nematic phase and hence the strength of the coupling between nematic and smectic-*A* order parameter and therefore the resultant pretransitional behavior can be investigated.

3.4.2. Thin prism technique

The thin prism technique [40] has been used to measure the extraordinary (n_e) and ordinary (n_o) refractive indices for all of the mixtures under study by probing a laser beam of wavelength λ = 632.8 nm. The variation

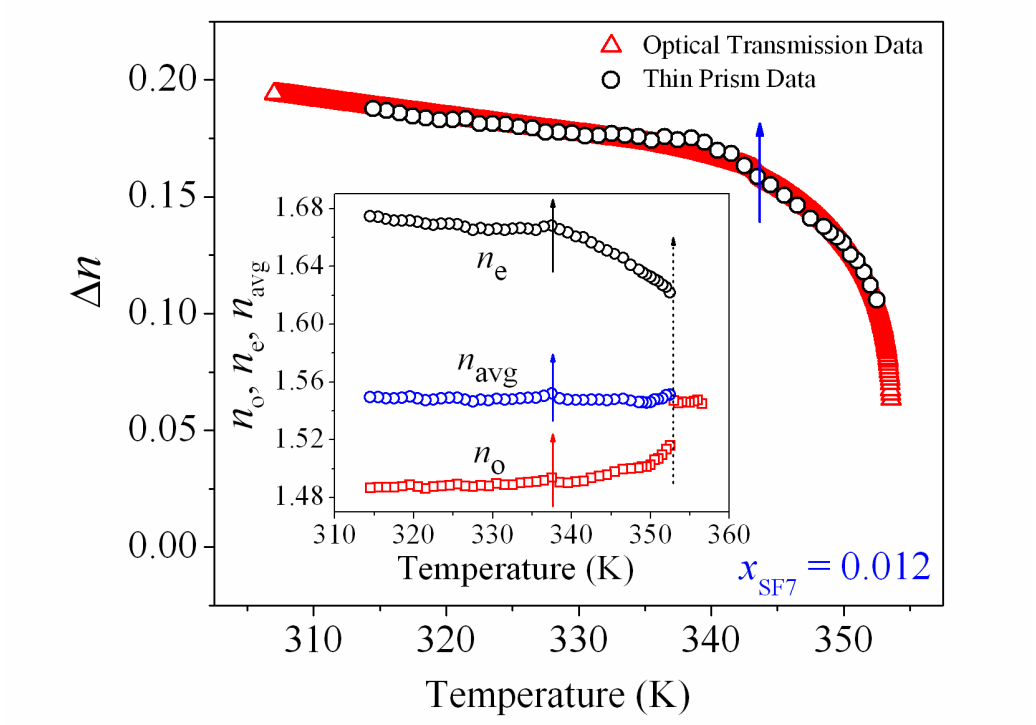

(a)

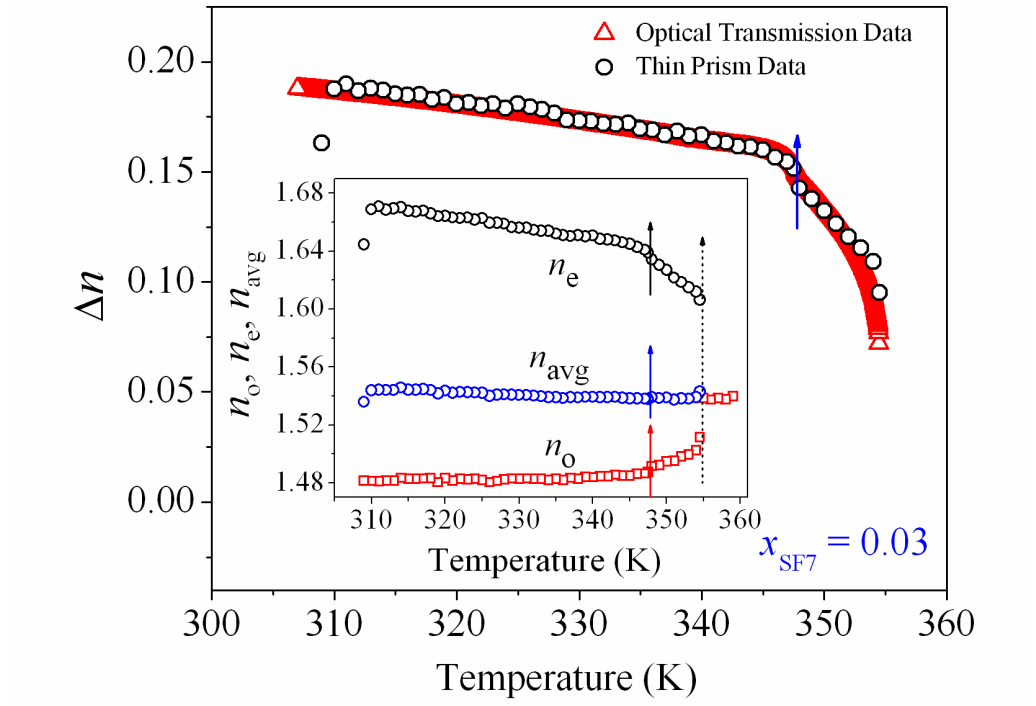

(b)

Figure 3.4. Refractive indices (n_e, n_o) and birefringence (Δn = n_e-n_o) as a function of temperature for (a) x_{SF7} = 0.012, (b) x_{SF7} = 0.03. Dashed arrow and solid arrows denote the isotropic–nematic (T_{IN}) and nematic–smectic-*A* (T_{NA}) transition temperatures respectively.

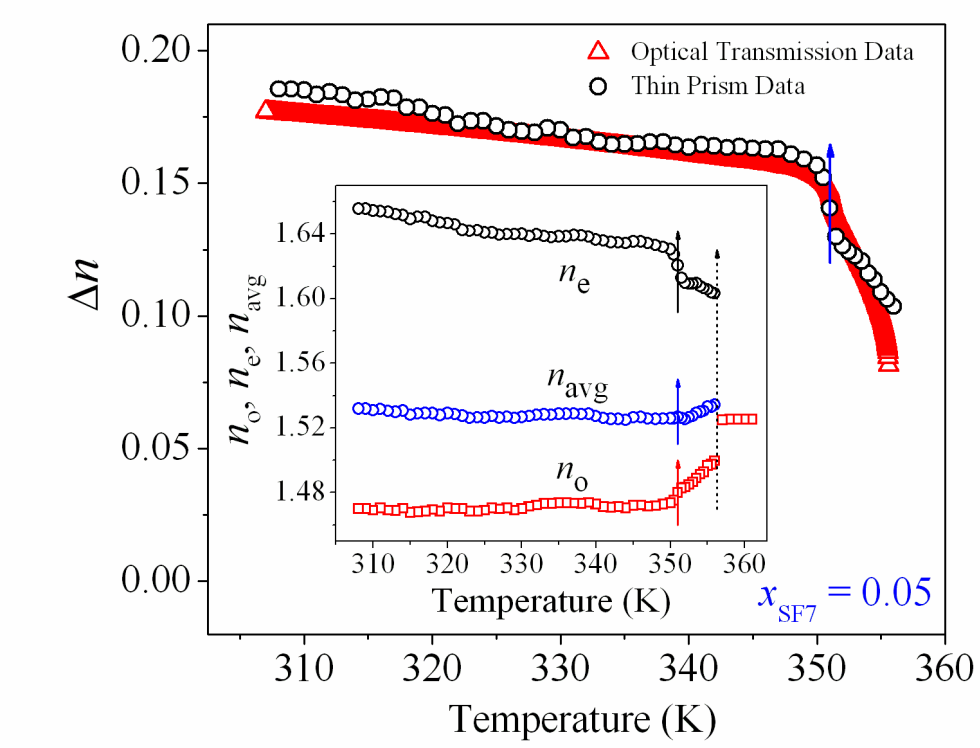

(c)

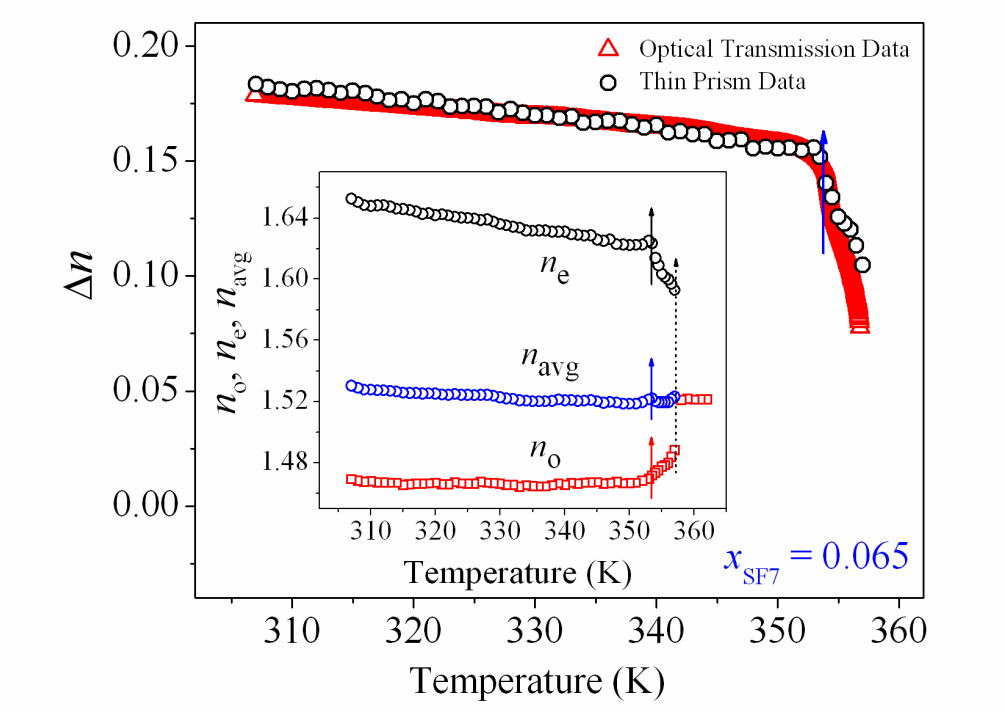

(d)

Figure 3.4 (cont'd). Refractive indices (n_e, n_o) and birefringence ($\Delta n = n_e - n_o$) as a function of temperature for (c) $x_{SF7} = 0.05$, (d) $x_{SF7} = 0.065$. Dashed arrow and solid arrows denote the isotropic–nematic (T_{IN}) and nematic–smectic-*A* (T_{NA}) transition temperatures respectively.

of two principal refractive indices (n_o, n_e) along with the average refractive index (n_{avg}) with temperature for four different mixtures are shown in inset of Fig. 3.4(a-d). These figures clearly reveals that the measured refractive index (n_{iso}) in the isotropic (*I*) phase is nearly invariant with respect to the change in temperature. But at the *I*–*N* phase transition, the refractive index splits into two parts, *i.e.*, one with higher and another with lower than the isotropic value correspond to the extraordinary (n_e) and ordinary (n_o) refractive indices respectively. The higher refractive index (n_e) is found to be strongly temperature dependent within the whole mesomorphic range while the ordinary component (n_o) is weakly dependent on temperature except in the vicinity of isotropic–nematic phase transition. Moreover, the n_o, n_e data do not show any pronounced change near the *N*–Sm-*A* transition for all the investigated mixtures. The temperature dependent variation of the optical birefringence ($\Delta n = n_e - n_o$) value for all of the investigated mixtures are also shown in the respective figures. It is quite evident that a relatively higher value of Δn in the Sm-*A* phase compared to *N* phase is due to the increase of molecular ordering, which results in an enhancement of the optical anisotropy. Nevertheless, the temperature variation of Δn in the Sm-*A* phase is comparatively sluggish compared to that in the nematic phase. Therefore, the measured Δn value reveals a quite well agreement obtained from both the optical transmission method and thin prism technique. In spite of such agreement, the Δn values obtained from high-resolution optical transmission technique are most efficient for further analysis owing to have small temperature interval between the successive data points.

3.5. Critical behavior at the *I*–*N* phase transition

In order to probe the critical behavior of the *I*–*N* phase transition, proper understanding of the scalar order parameter S(*T*) [41] associated with the local field around a molecule is necessary. Two most widely accepted models are – (i) the isotropic internal field model, proposed by Vuks, Chandrasekhar and

Madhusudana (VCM model) [42,43], and (ii) the anisotropic internal field model of Neugebauer, Maier and Saupe (NMS model) [44-46].

According to VCM model, molecular polarizability (α) of a mesogenic medium is linked with the birefringence (Δn) through the following relation:

$$\frac{\Delta\alpha}{\langle\alpha\rangle}\mathrm{S}(T) = \frac{\Delta(n^2)}{\langle n^2\rangle - 1} \tag{3.1}$$

where $\Delta(n^2) = n_e^2 - n_o^2$ is the anisotropy of the square of the refractive index and $\langle n^2\rangle = (n_e^2 + 2n_o^2)/3$, while n_e and n_o are the extraordinary and ordinary refractive indices respectively. The molecular polarizability anisotropy is termed as $\Delta\alpha = \alpha_l - \alpha_t$ and the mean polarizability $\langle\alpha\rangle = (\alpha_l + \alpha_t)/3$ where α_l and α_t are the longitudinal and transverse polarizabilities with respect to the long molecular axis, respectively. Moreover, to determine the temperature dependence of the nematic order parameter $S(T)$, the four-parameter power-law expression related to the mean-field theory for both the critical and tricritical character of a weakly first-order transition [18,47] has been used which can be expressed as:

$$S(T) = S^{**} + A\left|\left(1 - \frac{T}{T^{**}}\right)\right|^{\beta} \tag{3.2}$$

where β represents the order parameter critical exponent, A is a constant, T^{**} is the effective second order transition temperature below the clearing temperature (T_{IN}). This absolute limit of the superheating temperature in the nematic phase is found to be slightly higher than the observed *I–N* phase transition temperature (T_{IN}). Hence, at $T = T^{**}$, $S(T^{**}) = S^{**}$.

By introducing appropriate scaling condition and few approximations one can coupled both the Eq. (3.1) and Eq. (3.2) together and modified to [48-50]:

$$\Delta n = \zeta\left[S^{**} + (1 - S^{**})\left|\left(1 - \frac{T}{T^{**}}\right)\right|^{\beta}\right] \tag{3.3}$$

where, $\zeta = (\Delta\alpha/\alpha)[(n_I^2 - 1)/2n_I]$ and n_I is the refractive index in the isotropic phase (just above T_{IN}).

The critical anomaly near the *I–N* phase transition has been evaluated by using a fitting procedure to the temperature dependence of high-resolution optical birefringence data with a simple power-law formula as expressed in Eq. (3.3) [51,52]. Fig. 3.5 illustrates the fitting curves of Eq. (3.3) with Δn for the pure compound 8OCB along with the investigated mixtures and the corresponding fit parameters are listed in Table 3.1.

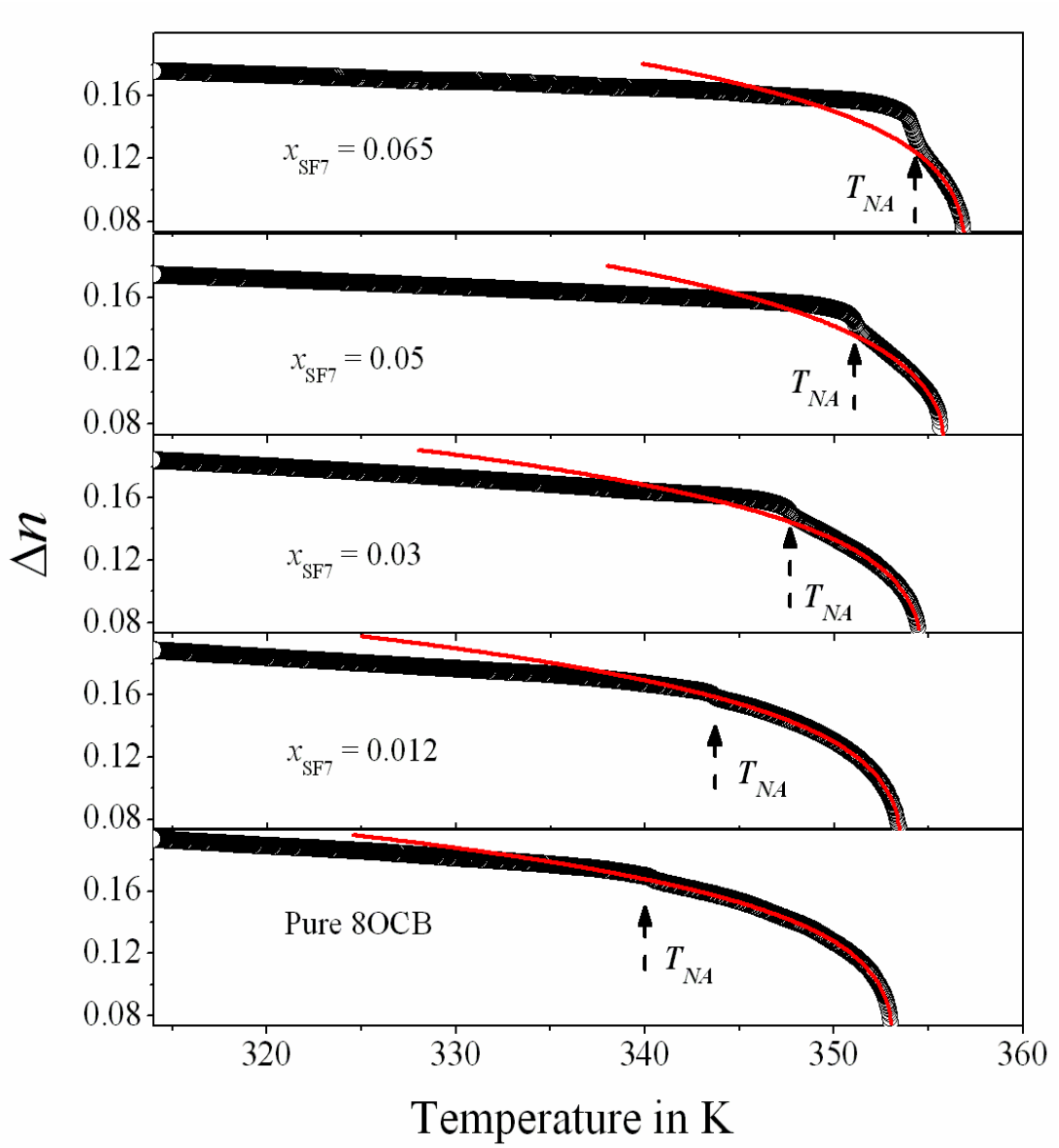

Figure 3.5. Variation of the temperature-dependent optical birefringence data for all the mixtures including pure 8OCB. Dashed arrow denotes the nematic–smectic-*A* (T_{NA}) transition temperature. The solid line is a fit to Eq. (3.3).

Table 3.1. Values of the fit parameters obtained from the four-parameter fit of the temperature dependence of Δ*n* to Eq. (3.3).

x_{SF7}	ζ	S^{**}	T^{**} *in K*	β	χ_v^2
0	0.336±0.025	0.099±0.012	353.15±0.64	0.248±0.075	1.01
0.012	0.344±0.004	0.084±0.026	353.60±0.16	0.248±0.014	1.24
0.03	0.337±0.104	0.080±0.045	354.68±2.38	0.249±0.028	1.33
0.05	0.356±0.062	0.058±0.042	356.09±2.20	0.250±0.051	1.49
0.065	0.353±0.054	0.087±0.031	356.96±1.80	0.253±0.018	1.62

The quality of the fits has been tested with the aid of the reduced error function χ_v^2, which is defined as the ratio of the variance of the fit (s^2) data to the variance of the experimental data (σ^2) [53],

$$\chi_v^2 = \frac{s^2}{\sigma^2} = \frac{1}{N-p}\sum_i \frac{1}{\sigma_i^2}\left(Q_i^{obs} - Q_i^{fit}\right)^2 \quad (3.4)$$

Here N is the total number of data points, p is the number of adjustable parameters, $Q_i^{fit}$is the i^{th} fit value corresponding to the measurement Q_i^{obs}, and σ^i is the standard deviation corresponding to Q_i^{obs}. For an ideal fit, χ_v^2 is unity but in general values ranging between 1 and 1.5 corresponds to good fits.

Moreover, the fitting procedure have been performed only in the stable nematic range excluding the region very close to the transitions where the pretransitional effect of both the *I*–*N* and *N*–Sm-*A* are pronounced. Hence for the mixture with small nematic range (~2.7 K) provides only 2 K of usable nematic range for the fitting. The fitted curves are represented by red lines in Fig. 3.5 extrapolating into the smectic-*A* phase. In the present investigated system, the obtained order parameter critical exponent (β) values lie in between 0.248 and 0.253 within a reasonable error limit. However, in case of three parameter Haller's method, reported β values are generally found less than 0.2, inconsistent with the nature of the weakly first-order character of the *I*–*N* phase transition [54]. Therefore, the four parameter power law expression approaches the theoretically predicted value better than the Haller's type expression as far

as the β value is concerned. According to tricritical hypothesis (TCH) of Keyes [16] and Anisimov *et al.* [17,18], the order parameter critical exponent endorse a value equal to 0.25 and hence the extracted β values in the present system are found to be concurred with the theoretically predicted tricritical value. Therefore, this study confirms the tricritical nature of the *I–N* phase transition and discards the possibility of lower β values.

3.6. Critical behavior at the *N*−Sm-*A* phase transition

The *N*−Sm-*A* phase transition is accompanied with an enhancement of orientational ordering, motivated by coupling between nematic and smectic order parameters. However, the temperature-dependent smectic-*A* order parameter is related to specific heat capacity exponent α as [21,55,56]:

$$\langle|\psi|^2\rangle = U \pm V^{\pm}\left|\left(\frac{T}{T_{NA}} - 1\right)\right|^{\kappa} \tag{3.5}$$

where κ = 1-α, and the ± signs refer to quantities above and below the *N*−Sm-*A* phase transition temperature (T_{NA}) respectively. According to mean field model, the quantity (S-S_0) is proportional to $\langle|\Psi|^2\rangle$, where S_0 is the nematic order parameter in absence of any smectic ordering [21,57]. Moreover, the nematic order parameter (S) is also proportional to Δn. Hence, by investigating the behavior of optical birefringence in the vicinity of *N*−Sm-*A* phase transition, an identical power-law divergence behavior and a critical exponent (α') identical to specific heat capacity critical exponent (α) can be established.

In an effort to investigate this critical region and as well as to reveal the unique aspects of the *N*−Sm-*A* phase transition the high-resolution optical birefringence (Δn) data have been used to obtain an insight into the critical behavior at the *N*−Sm-*A* phase transition. Although the Δn curves do not accompanied by any visible discontinuity at the *N*−Sm-*A* phase transition, a quantity $n' = -\,d(\Delta n)/dT$, *i.e.*, the first order temperature derivative of Δn has been used to identify the exact transition temperature. The quantity n′ has also been found to be related to specific heat capacity anomaly [58] and may be

utilized to investigate the critical fluctuations associated with that transition. But in this case, due to small temperature interval between the successive data points, the numerically obtained temperature derivative of Δn is significantly scattered. Hence, it is reasonable to introduce another differential quotient Q(T), defined as [51,52,59]

$$\mathrm{Q}(T) = -\frac{\Delta n(T) - \Delta n(T_{NA})}{T - T_{NA}} \tag{3.6}$$

where $\Delta n(T_{NA})$ is the birefringence value at the N−Sm-A phase transition temperature (T_{NA}). The quantities n′ and Q(T) share the identical power-law behavior and hence are characterized by the same critical exponent α' describing the transitional fluctuations. In an attempt to obtain an impression of the limiting behavior of the quotient Q(T) at the N−Sm-A phase transition, fits to the following renormalization group expression including the corrections to scaling term have been performed [59,60]:

$$\mathrm{Q}(T) = A^{\pm}|\tau|^{-\alpha'}(1 + D^{\pm}|\tau|^{\Delta}) + E(T - T_{NA}) + B \tag{3.7}$$

where, $\tau = (T\text{-}T_{NA})/T_{NA}$, ± denote terms above and below T_{NA}, $A^{\pm}$ denotes the critical amplitudes, $D^{\pm}$ are the coefficients of the first corrections-to-scaling terms, α' is the effective critical exponent similar to specific heat capacity critical exponent, Δ is the first corrections-to-scaling exponent and B represents the combined critical and regular backgrounds while the term $E(T\text{-}T_{NA})$ stands for a temperature dependant part of the regular background contribution. The theoretically predicted value of Δ is 0.524 for a 3D-XY case [61,62] and in this analysis it is set fixed at 0.5 without any further variation. The temperature dependence of the quotient Q(T) for four different mixtures under investigation along with that for pure 8OCB are shown in Fig. 3.6. Fits to Eq. (3.7) on either sides of the N−Sm-A transition temperature are depicted as solid red lines in the same figure. The values of the fit parameters are listed in Table 3.2. During the fit process, few data points very close to the transition have been excluded to avoid the error resulting from the experimental uncertainty. Fits have been carried out for different temperature ranges and that interval for which the fit

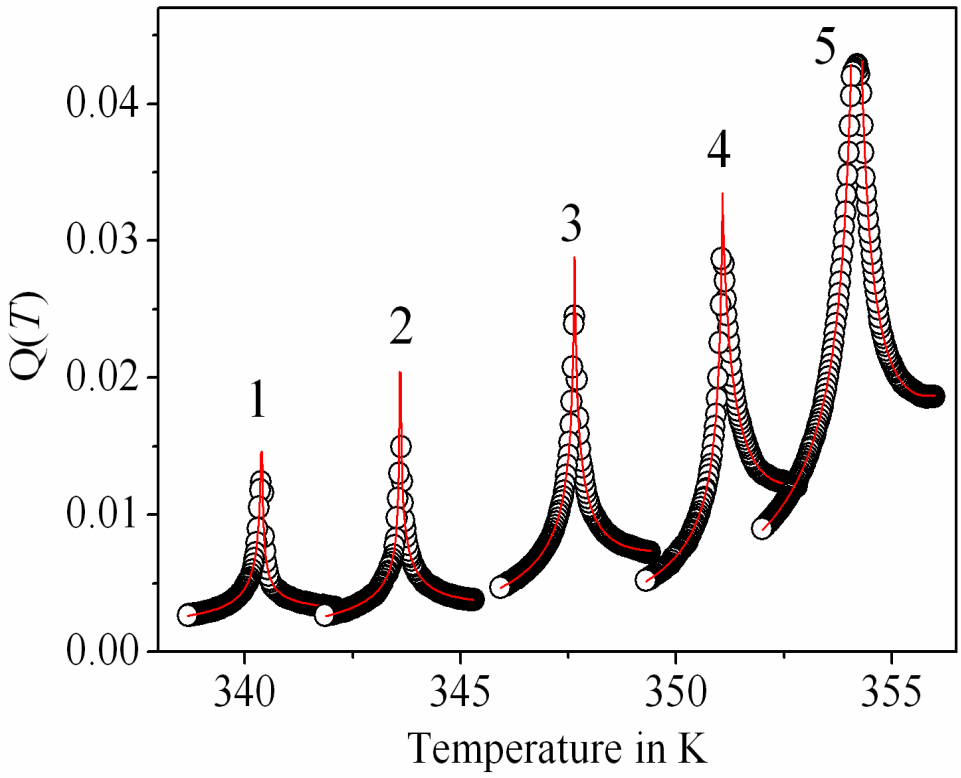

Figure 3.6. Temperature dependent variation of the quotient Q(*T*) in the vicinity of *N*−Sm-*A* phase transition for different mole fractions of SF7. Data are arranged in sequence of increasing mole fraction of SF7 from left to right with 1: 8OCB; 2: x_{SF7} = 0.012; 3: x_{SF7} = 0.03; 4: x_{SF7} = 0.05; 5: x_{SF7} = 0.065. The solid lines are fit to Eq. (3.7).

Table 3.2. Results corresponding to the best fit for Q(*T*) near the *N*−Sm-*A* phase transition obtained in accordance with Eq. (3.7) and related χ_v^2 values associated with the fits. $|\tau|_{max}$ presents the upper limit of reduced temperature considered for these fits.

x_{SF7}	α'	A^-/A^+	D^-/D^+	$\|\tau\|_{max}$	χ_v^2
0.00	0.201 ± 0.005	0.87 ± 0.005	0.83 ± 0.002	5×10^{-3}	1.15
0.012	0.278 ± 0.003	0.97 ± 0.001	0.98 ± 0.003	5×10^{-3}	1.21
0.03	0.379 ± 0.006	1.00 ± 0.004	1.00 ± 0.015	5×10^{-3}	1.55
0.05	0.440 ± 0.010	0.88 ± 0.032	0.99 ± 0.024	5×10^{-3}	1.30
0.065	0.485 ± 0.019	1.01 ± 0.066	0.99 ± 0.056	5×10^{-3}	1.71

parameters remain practically stable for a small change in temperature range along with a minimum regular pattern in the residuals, have been considered [63]. The quality of the fits has been tested with the aid of the reduced error function χ_v^2. In our present investigation, χ_v^2 values lie in the range between 1.15 and 1.71, which indicates a consistent fit of the temperature dependance of the quotient Q(T) to the model expression (3.7) considered. In each fit, from the temperature dependence of d(Δn)/dT, the transition temperature was first isolated and then kept fixed. This reduces the instability appearing in the least-squares minimization significantly.

The concentration dependence of the extracted effective critical exponent α' values for the present investigated mixtures including that for the pure 8OCB is displayed in Fig. 3.7 while the variation of the same against the McMillan ratio (*i.e.*, T_{NA}/T_{IN}) is illustrated in Fig. 3.8. The measured value of the critical exponent α' for pure 8OCB has been found to be 0.201±0.005, which again is consistent with those reported in literature [64-66]. It has been observed that with increasing hockey stick compound concentration, α' increases monotonically from 0.278±0.003 for x_{SF7} = 0.012 to 0.485±0.019 for x_{SF7} = 0.065, *i.e.*, the yielded values are in between those for a 3D-*XY* system (*i.e.*, $\alpha_{3D\text{-}XY}$ = – 0.007) and for the tricritical case (*i.e.*, α_{TCH} = 0.5). Hence, non-universal values have been obtained for the effective critical exponent α' and hence indicating a crossover character for the *N*−Sm-*A* phase transitions in the present investigated mixtures. Moreover, throughout the concentration range, both the quotients A^-/A^+ and D^-/D^+ remain more or less equal to unity, indicating a symmetry of the Q(T) wings in both the Sm-*A* and *N* phases.

Investigation of Fig. 3.7 and Fig. 3.8 reveals that an extrapolation of a quadratic fit to extracted α' values results a crossover from second order to first order character for a composition $x_{SF7} \sim 0.072$ with $\alpha' = 0.5$, with the associated McMillan ratio (*i.e.*, T_{NA}/T_{IN}) being 0.994. Therefore, the tricritical point (TCP) for the investigated binary system is reached approximately at $x_{SF7} \sim 0.072$. It is

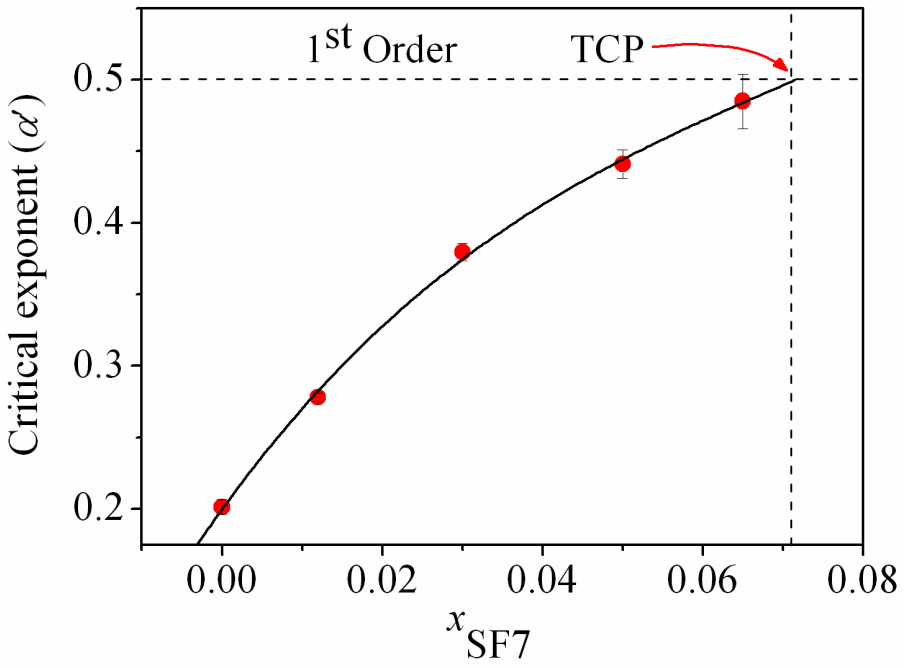

Figure 3.7. Concentration dependence of the effective critical exponent (α') obtained by fitting Q(T) to Eq. (3.7). The vertical dashed line corresponds to the tricritical point (TCP). The solid line is a 2nd order polynomial fit to the data.

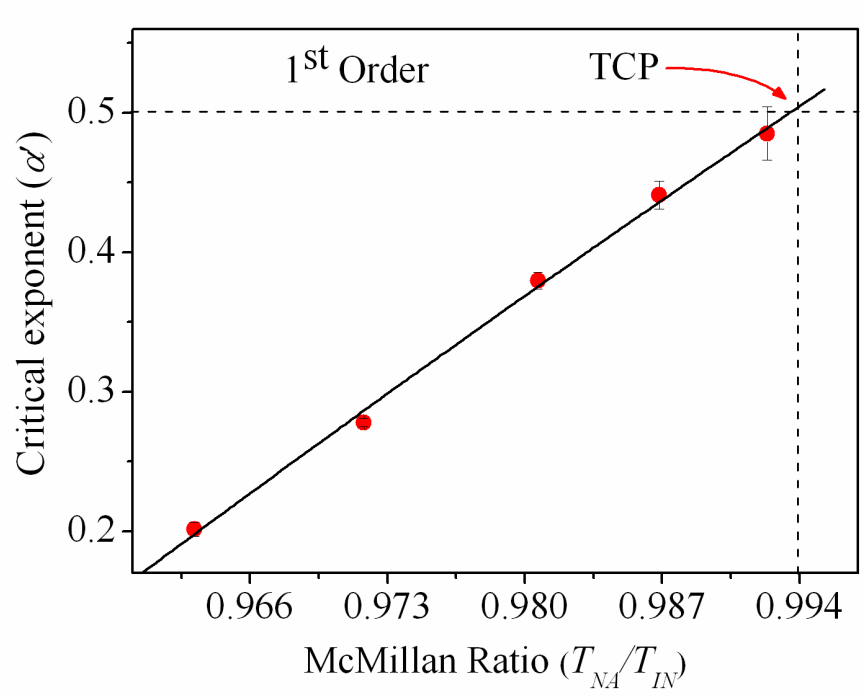

Figure 3.8. Variation of effective critical exponent (α') with McMillan ratio (T_{NA}/T_{IN}). The vertical dashed line corresponds to the tricritical point (TCP). The solid line is a linear fit to the data.

quite clear that addition of this angular mesogenic compound (SF7) in the calamitic medium (8OCB) strengthens the coupling between the nematic (S) and smectic (Ψ) order parameters which again lead to a decrease in the nematic width. Additionally this coupling becomes considerably stronger for a relatively small increase in concentration of the angular mesogenic compound in the mixtures. Such an outcome is possibly due to modification in effective intermolecular interaction and the local molecular ordering in the host medium due to the introduction of the hockey stick-shaped dopant, which again drives the transition from second order to first order character [67].

Moreover, below the *N*–Sm-*A* transition an analysis has also been carried out to characterize the critical behavior using an expression related to the reduced temperature (τ') [67], as follows:

$$\Delta n = A|\tau'|^{\lambda} + B|\tau'| + C \tag{3.8}$$

where, $|\tau'| = |1 - T/T_{NA}|$ is the reduced temperature, A is a constant and $B|\tau'|$ presents the temperature-dependent part of the regular background, whereas C is the combined critical and regular background term and λ gives the critical coefficient. A representation of reduced temperature dependent value of Δn below the *N*–Sm-*A* phase transition for all the mixtures has been presented in Fig. 3.9, while the fits to Eq. (3.8) has also been included on corresponding data points by red solid lines. The fit parameters so obtained are listed in Table 3.3. Range of τ' has been taken to a value from 0 to 0.007 and this effectively made a temperature range 2.5 K below the *N*–Sm-*A* phase transition. It has been observed from Table 3.3 that the exponent λ assumes a value of 0.638 ± 0.024 for pure 8OCB and with increasing concentration of SF7 the λ value decreases to 0.506 ± 0.008 for x_{SF7} = 0.065. Furthermore, for a long-range ordered system, scaling theory requires $\lambda = 2\beta$, where β is the critical exponent related to limiting behavior of order parameter at the *N*–Sm-*A* phase transition. Additionally, by considering the Landau–de Gennes theory this exponent λ is

equal to (1-α) for few mesogenic systems [56] and for a number of other mesogens it has been seen that λ < (1-α) [56].

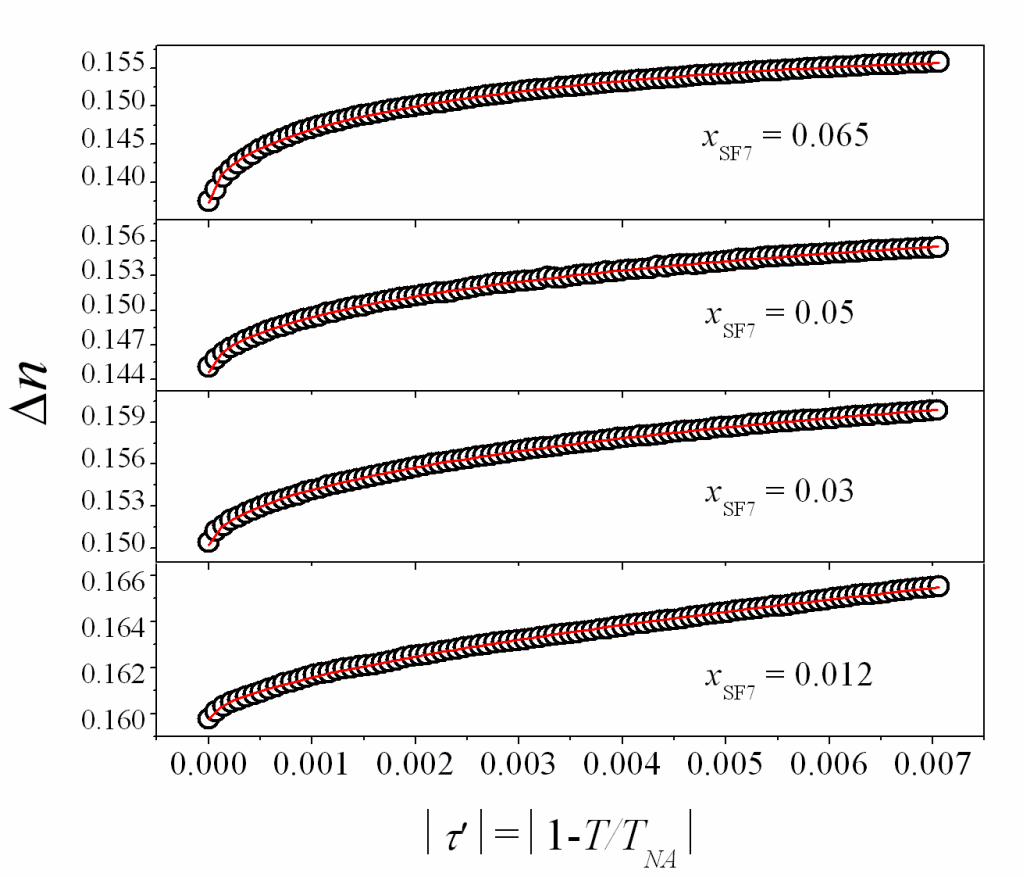

Figure 3.9. Plot of optical birefringence as a function of reduced temperature $|\tau'| = |1\text{-}T/T_{NA}|$ for different mixtures. The solid lines are fit to Eq. (3.8).

Table 3.3. Values of the fit parameters obtained from the fit of the temperature dependence of Δn to Eq. (3.8).

x_{SF7}	A	λ	β' (= λ/2)	B	C	χ_v^2
0	0.094±0.043	0.638±0.024	0.319±0.012	0.202±0.094	0.16818	1.6
0.012	0.101±0.019	0.587±0.027	0.294±0.013	0.025±0.056	0.15981	1.34
0.03	0.218±0.015	0.562±0.009	0.281±0.005	-0.540±0.047	0.15022	1.05
0.05	0.223±0.022	0.537±0.014	0.268±0.007	-0.664±0.075	0.14461	1.22
0.065	0.373±0.172	0.506±0.008	0.253±0.004	-1.705±0.543	0.1373	1.41

Combining all these conditions, it can be predicted that the λ values should lie in a range of $2\beta \leq \lambda \leq (1-\alpha)$. In the present system, it is clearly observed from Tables 3.2 and 3.3 that the extracted λ values are relatively smaller than the computed $(1-\alpha)$ values, whereas α is considered as α' (Table 3.2). Again, if the extracted $\lambda/2$ values are plotted against McMillan ratio, extrapolation to a quadratic fit of these values assigned a tricritical point at a McMillan ratio of ~ 0.994, which is almost equal value as obtained by the fit to α' values, shown in Fig. 3.10. Therefore, it can be safe to assume $\beta \cong \lambda/2 = \beta'$. A comparison of the obtained values of β' for an another binary system [67] comprising a different hockey stick-shaped compound 4-(3-*n*-decyloxy-2-methyl phenyliminomethyl) phenyl 4-*n*-dodecyloxycinnamate (H-22.5) and the rod-like mesogen octylcyanobiphenyl (8CB) has been included in the present system on the same figure and reveals a close agreement of the obtained β'

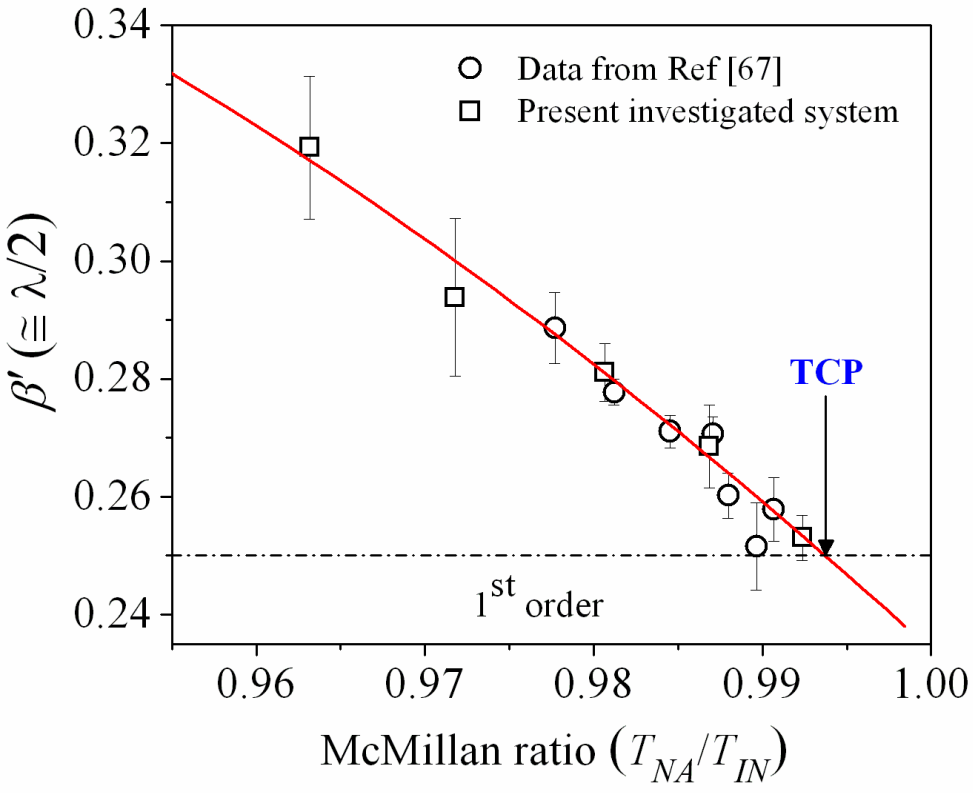

Figure 3.10. Variation of order parameter critical exponent (β') value with McMillan ratio (T_{NA}/T_{IN}). The solid line is a second-order polynomial fit to the data.

values for both the systems. Hence, a crossover behavior of critical exponents (α', β') within the limit of uncertainty has been established in the present investigated system.

In an earlier investigation [67] on an another binary system comprising of a different hockey stick-shaped mesogen H-22.5 with a lateral methyl group and the rod-like compound 8CB, the effective order parameter critical exponent (β) for the *I–N* phase transition has been found to be in agreement with the tricritical hypothesis. On the other hand, a crossover character has been revealed for the *N*−Sm-*A* phase transition, with the related effective critical exponent (α') being non-universal in nature. Furthermore, for the *N*−Sm-*A* phase transition, the extracted critical character has usually been found to be sensitive to the width of the nematic phase range. The nematic width has also been found to be shrunk considerably with enhancing hockey stick molecule concentration along with the related effective critical exponent α', attaining a value of 0.460 ± 0.016 for a mole-fraction 0.08 of the hockey stick-shaped compound. Due to a relatively small width of the nematic phase (~ 7 K) in the host 8CB, it became possible to investigate the critical exponent variation over a relatively narrow range (in between $\alpha' = 0.319$ and 0.46). Now in the present study, the compound 8OCB possesses a comparatively larger nematic width (~ 13 K) and hence it is expected that the dependence of α' on the McMillan ratio can be investigated on a relatively broad scale. However, in the present mixtures α' has been found to vary between 0.278±0.003 and 0.485±0.019 depending on the dopant concentration and hence the variation range is marginally greater than that in the previous study. Furthermore, this variation is manifested over a relatively short range of concentration variation of the angular dopant in the host mesogen (*i.e.*, x_{SF7} = 0.012 to 0.065) as compared to the earlier case. Such a strong augmentation in the exponent α' certainly indicates a relatively rapid growth in the local molecular ordering and hence the coupling between the order parameters S and Ψ. A further indication

of such increase in coupling is the rather steep slope of the phase boundary, a measure of which again can be manifested by calculating related average $d(T_{NA})/dx$ value. In the present case, the slope has been found to be ~ 212 K which again is comparatively greater than the previous value ~ 169 K. Furthermore, the concentration dependence of the nematic width has also been found to demonstrate a relatively sharp decrease (slope ~ 150 K) compared to the former study (slope ~ 50 K). Such an outcome is perhaps due to the fine structural dissimilarity between SF7 and H-22.5.

Both the hockey stick-shaped compounds possess a more or less identical molecular configuration except the presence of a lateral methyl group in the obtuse angle between the *meta*-alkyloxy chain attached to the terminal phenyl ring and the azomethine connecting group in H-22.5. Such a substitution has been observed to impart a dramatic influence on the phase behavior of H-22.5 causing the emergence of a nematic phase in a small temperature range [68]. Steric interactions between the methyl group and the

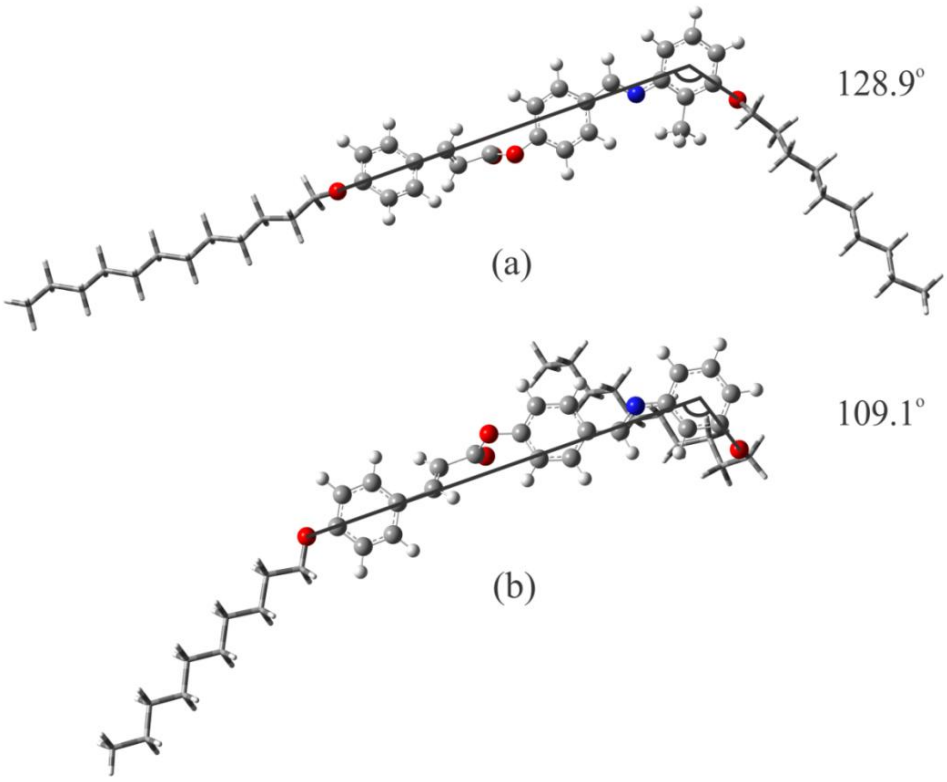

Fig. 3.11. Optimized molecular structure of (a) H-22.5, (b) SF7.

neighboring alkoxy chain in the *meta*-position in H-22.5 perhaps induce a more rod-like shape compared to SF7 which again is facilitated in a relatively less augmentation of the local molecular order and hence in a rather less strengthening of the coupling between S and Ψ. In an attempt to gain an idea, the molecular bend-angle of both the compounds has been calculated using Gauss View. The bend-angle appeared to be 128.9^{o} and 109.1^{o} for compounds H-22.5 and SF7 (as shown in Fig. 3.11) respectively which again certainly imply more rod-like appearance for H-22.5.

3.7. Conclusion

In this work, systematic measurements have been carried out on high-resolution temperature dependence of optical birefringence for a binary system, consisting of a hockey stick-shaped liquid crystal compound, 4-(3-decyloxyphenyliminomethyl) phenyl 4-decyloxycinnamate (SF7) and the rod like 4-cyano-4′-octyloxybiphenyl (8OCB). The measured optical birefringence (Δn) values demonstrate a quite well consistency obtained from both the optical transmission method and thin prism technique. However, due to quite high resolution as well as large number of data points, the birefringence value obtained from optical transmission technique are found to be rather successful in describing the transitional behavior more precisely at the *I*–*N* and *N*−Sm-*A* phase transitions in all the investigated mixtures. The temperature dependence of birefringence exhibits a sharp change at the *I*–*N* phase transition for all of the investigated mixtures. The extracted order parameter critical coefficient β has found to be very close to the theoretically predicted tricritical value (β = 0.25) for the *I*–*N* phase transition. Furthermore, a continuous change of Δn at the *N*−Sm-*A* transition has been observed, indicating a second order nature of that transition. An enhancement in hockey stick-shaped compound in the mixtures lead to a significant decrease in the nematic width, *i.e.*, it stabilizes the low temperature smectic phase. A noticeable pretransitional behavior has been observed in the temperature dependence of Δn in a certain temperature

range above and below the *N*−Sm-*A* transition. The differential quotient Q(*T*) exhibits a diverging character in the vicinity of *N*−Sm-*A* transition which reveals a good conformity with a renormalization-group model. The related effective critical exponent (α'), describing the critical fluctuations at that transition, has appeared to be non-universal in nature. The α' values follow a monotonic enhancement against the concentration variation of the hockey stick-shaped compound, where an extension of fit to the exponents results a crossover to first order nature of the *N*−Sm-*A* phase transition for a McMillan ratio of 0.994 which again is in close agreement with the reported value for the mixtures of similar mesogenic systems. Moreover, a critical exponent (β') identical to the order parameter critical exponent β at the *N*–Sm-*A* phase transition has been found to be concentration dependent and reveals a good agreement with the same obtained from another binary system consisting of a hockey stick-shaped compound H-22.5 and a rod-like mesogen 8CB. One interesting fact emerging out from this study is that the molecular bend of the angular mesogenic dopant imparts an influence on the phase-character of the mixtures involving angular mesogenic dopant. From the observations, it is clear that an enhanced molecular bend leads to a relatively stronger S – Ψ coupling and a sharp decrease in the nematic width. This again manifest in a rapid approach towards the first order nature of the *N*−Sm-*A* phase transition. The exact description, portraying the dependence of order character of the *N*−Sm-*A* phase transition on the molecular bend of mesogenic dopant requires further investigations involving mesogenic systems with varied dopant–host combinations.

References:

[1] J. Thisayukta, H. Niwano, H. Takezoe, and J. Watanabe, *J. Am. Chem. Soc.*, **124**, 3354 (2002).

[2] M. Nakata, Y. Takanishi, J. Watanabe, and H. Takezoe, *Phys. Rev. E*, **68**, 041710 (2003).

[3] E. Gorecka, M. Čepič, J. Mieckowski, M. Nakata, H. Takezoe, and B. Žekš, *Phys. Rev. E*, **67**, 061704 (2003).

[4] R.E. Gorecka, M. Nakata, J. Mieczkowski, Y. Takanashi, K. Ishikawa, J. Watanabe, H. Takezoe, S.H. Eichhorn, and T.M. Swager, *Phys. Rev. Lett.*, **85**, 2526 (2000).

[5] K. Kishikawa, N. Muramatsu, S. Kohmoto, K. Yamaguchi, and M. Yamamoto, *Chem. Mater.*, **15**, 3443 (2003).

[6] C.K. Lee, J.H. Kim, E.J. Choi, W.C. Zin, and L.C. Chien, *Liq. Cryst.*, **28**, 1749 (2001).

[7] E.J. Choi, X. Cui, W.C. Zin, C.W. Ohk, T.K. Lim, and J.H. Lee, *Chem. Phys. Chem.*, **8**, 1919 (2007).

[8] R. Prathibha, N.V. Madhusudana, and B.K. Sadashiva, *Science*, **288**, 2184 (2000).

[9] B. Kundu, R. Pratibha, and N.V. Madhusudana, *Phys. Rev. Lett.*, **99**, 247802 (2007).

[10] P. Sathyanarayana, M. Mathew, Q. Li, V.S.S. Sastry, B. Kundu, K.V. Le, H. Takezoe, and S. Dhara, *Phys. Rev. E*, **81**, 010702 (2010).

[11] A. Chakraborty, M.K. Das, B. Das, A. Lehmann, and C. Tschierske, *Soft Matter*, **9**, 4273 (2013).

[12] T. Otani, F. Araoka, K. Ishikawa, and H. Takezoe, *J. Am. Chem. Soc.*, **131**, 12368 (2009).

[13] C. Zhu, D. Chen, Y. Shen, C.D. Jones, M.A. Glaser, J.E. Maclennan, and N.A. Clark, *Phys. Rev. E*, **81**, 011704 (2010).

[14] P.G. de Gennes, and J. Prost, in *The Physics of Liquid Crystals*, Oxford University Press, Oxford (1993).

[15] W. Maier, and A. Saupe, *Z. Naturforsch. A*, **13a**, 564 (1958); **14a**, 882 (1959).

[16] P.H. Keyes, *Phys. Lett. A*, **67**, 132 (1978).

[17] M.A. Anisimov, S.R. Garber, V.S. Esipov, V.M. Mamnitskii, G.I. Ovodov, L.A. Smolenko, and E.L. Sorkin, *Sov. Phys. JETP*, **45**, 1042 (1977).

[18] M.A. Anisimov, *Mol. Cryst. Liq. Cryst. Inc. Nonlinear Opt.*, **162**, 1 (1988).

[19] K.K. Kobayashi, *Phys. Lett. A*, **31**, 125 (1970); *J. Phys. Soc. Jpn.*, **29**, 101 (1970).

[20] W.L. McMillan, *Phys. Rev. A*, **4**, 1238 (1971).

[21] P.G. de Gennes, *Mol. Cryst. Liq. Cryst.*, **21**, 49 (1973).

[22] H. Marynissen, J. Thoen, and W. vanDael, *Mol. Cryst. Liq. Cryst.*, **97**, 149 (1983).

[23] M.E. Huster, K.J. Stine, and C.W. Garland, *Phys. Rev. A*, **36**, 2364 (1987).

[24] H. Marynissen, J. Thoen, and W. vanDael, *Mol. Cryst. Liq. Cryst.*, **124**, 195 (1985).

[25] K.J. Stine, and C.W. Garland, *Phys. Rev. A*, **39**, 3148 (1989).

[26] S.K. Sarkar, and M.K. Das, *RSC Adv.*, **4**, 19861 (2014).

[27] S.K. Sarkar, and M.K. Das, *J. Mol. Liq.*, **199**, 415 (2014).

[28] P. Cusmin, M.R. de la Fuente, J. Salud , M.A. Pérez-Jubindo , S. Diez-Berart, and D.O. López, *J. Phys. Chem. B.*, **111**, 8974 (2007).

[29] C.W. Garland, and G. Nounesis, *Phys. Rev. E*, **49**, 2964 (1994).

[30] J. Thoen, H. Marynissen, and W. Van Dael, *Phys. Rev. A*, **26**, 2886 (1982).

[31] J. Thoen, *Int. J. Mod. Phys. B*, **09**, 2157 (1995).

[32] P. Cusmin, J. Salud, D.O. López, M.R. de la Fuente, S. Diez, M.A. Pérez-Jubindo, M. Barrio, and J.L. Tamarit, *J. Phys. Chem. B.*, **110**, 26194 (2006).

[33] B.I. Halperin, T.C. Lubenski, and S.K. Ma, *Phys. Rev. Lett.*, **32**, 292 (1974).

[34] G. Sarkar, B. Das, M.K. Das, U. Baumeister, and W. Weissflog, *Mol. Cryst. Liq. Cryst.*, **540**, 188 (2011).

[35] A. Saipa, and F. Giesselmann, *Liq. Cryst.*, **29**, 347 (2002).

[36] G. Sarkar, M.K. Das, R. Paul, B. Das, and W. Weissflog, *Phase Transit.*, **82**, 433 (2009).

[37] T. Scharf, in *Polarized Light in Liquid Crystals and Polymers*, Wiley, Hoboken, NJ, (2007).

[38] A. Prasad, and M.K. Das, *J. Phys.: Condens. Matter*, **22**, 195106 (2010).

[39] P.G. de Gennes, *Solid State Commun.*, **10**, 753 (1972).

[40] A. Prasad, and M.K. Das, *Phase Transit.*, **83**, 1072 (2010).

[41] W. Maier, and A. Saupe, *Z. Naturforsch. A*, **13a**, 564 (1958); **14a**, 882 (1959).

[42] M. F. Vuks, *Opt. Spectrosc.*, **20**, 361 (1966).

[43] S. Chandrasekhar, and N.V. Madhusudana, *J. Phys.* (*Paris*), **30**, C4-24 (1969).

[44] H.E.J. Neugebauer, *Can. J. Phys.*, **32**, 1 (1954).

[45] A. Saupe, and W. Maier, *Z. Naturforsch. A*, **16a**, 816 (1961).

[46] H.S. Subramhanyam, and D. Krishnamurthi, *Mol. Cryst. Liq. Cryst.*, **22**, 239 (1973).

[47] J. Thoen, and G. Menu, *Mol. Cryst. Liq. Cryst.*, **97**, 163 (1983).

[48] I. Chirtoc, M. Chirtoc, C. Glorieux, and J. Thoen, *Liq. Cryst.*, **31,** 229 (2004).

[49] S. Yildiz, H. Özbek, C. Glorieux, and J. Thoen, *Liq. Cryst.*, **34,** 611 (2007).

[50] S. Erkan, M. Çetinkaya, S. Yildiz, and H. Özbek, *Phys. Rev. E*, **86**, 041705 (2012).

[51] H.E. Stanley, in *Introduction to Phase Transitions and Critical Phenomena*, Clarendon, Oxford, (1971).

[52] R. Brout, in *Phase Transitions*, Benjamin, New York, (1965).

[53] P. R. Bevington, and D.K. Robinson, in *Data Reduction and Error Analysis for the Physical Sciences*, McGraw-Hill, New York (2003).

[54] I. Haller, *Progr. Solid State Chem.*, **10**, 103 (1975).

[55] M.E. Fisher, and A. Aharony, *Phys. Rev. Lett.*, **31**, 1238 (1973).

[56] K.K. Chan, M. Deutsch, B.M. Ocko, P.S. Pershan, and L.B. Sorensen, *Phys. Rev. Lett.*, **54**, 920 (1985).

[57] K.-C. Lim, and J.T. Ho, *Phys. Rev. Lett.*, **40**, 944 (1978).

[58] A.V. Kityk, and P. Huber, *Appl. Phys. Lett.*, **97**, 153124 (2010).

[59] M.C. Cetinkaya, S. Yildiz, H. Ozbek, P. Losada-Perez, J. Leys, and J. Thoen, *Phys. Rev. E*, **88**, 042502 (2013).

[60] C.W. Garland, in *Liquid Crystals: Experimental Study of Physical Properties and Phase Transitions*, S. Kumar (Ed.), Cambridge University Press, Cambridge (2001).

[61] C. Bagnuls, and C. Bervillier, *Phys. Rev. B*, **32**, 7209 (1985).

[62] C. Bagnuls, C. Bervillier, D.I. Meiron, and B.G. Nickel, *Phys. Rev. B*, **35**, 3585 (1987).

[63] J.A. Potton, and P.C. Lanchester, *Phase Transit.*, **6**, 43 (1985).

[64] M.K. Das, P.C. Barman, and S.K. Sarkar, *Eur. Phys. J. B*, **88**, 175 (2015).

[65] G.B. Kasting, K.J. Lushington, and C.W. Garland, *Phys. Rev. B*, **22**, 321 (1980).

[66] G. Cordoyiannis, C.S.P. Tripathi, C. Glorieux, and J. Thoen, *Phys. Rev. E*, **82**, 031707 (2010).

[67] A. Chakraborty, S. Chakraborty, and M.K. Das, *Phys. Rev. E*, **91**, 032503 (2015).

[68] A. Chakraborty, B. Das, M.K. Das, S. Findeisen-Tandel, M.-G. Tamba, U. Baumeister, H. Kresse, and W. Weissflog, *Liq. Cryst.*, **38**, 1085 (2011).